JARS Journal of Applied Remote Sensing

RESEARCH PAPER

Spectral index for estimating leaf water content across diverse plant species using multiple viewing angles

Qazi Muhammad Yasir,[a,b,*] **Zhijie Zhang**,[c,*] **Jintong Ren**,[d] **Guihong Wang**,[d,e] **Muhammad Naveed**,[f] **Zahid Jahangir**,[g] **and Atta-ur-Rahman**[h]

[a]University of Limerick, Mary Immaculate College, Department of Geography, Limerick, Ireland
[b]Chinese Academy of Sciences, Aerospace Information Research Institute, Key Laboratory of Digital Earth Science, Beijing, China
[c]Utah State University, Quinbey College of Natural Resources, Department of Environment and Society, Logan, Utah, United States
[d]Guizhou University of Engineering Science, Bijie, China
[e]Southwest University, College of State Governance, Chongqing, China
[f]Northeast Normal University, Ministry of Education, School of Geographical Sciences, Key Laboratory of Geographical Processes and Ecological Security in Changbai Mountains, Changchun, China
[g]Wuhan University, Key Laboratory of Information Engineering in Surveying, Mapping and Remote Sensing, Wuhan, China
[h]University of Peshawar, Department of Geography and Geomatics, Peshawar, Pakistan

ABSTRACT. Understanding the impact of climate change on Earth presents a significant scientific challenge. Monitoring changes in terrestrial ecosystems, including leaf water content, is essential for assessing plant transpiration, water use efficiency, and physiological processes. Optical remote sensing, utilizing multi-angular reflectance measurements in the near infrared and shortwave infrared wavelengths, offers a precise method for estimating leaf water content. We propose and evaluate a new index based on multi-angular reflection, using 256 leaf samples from 10 plant species for calibration and 683 samples for validation. Hyperspectral indices derived from multi-angular spectra were assessed, facilitating efficient leaf water content analysis with minimal time and specific bands required. We investigate the relationship of leaf water content using spectral indices and apply linear and nonlinear regression models to calibration data, resulting in two indices for each indicator. The newly proposed indices, $(R_1 - R_2)/(R_1 - R_3)$ for linear and $(R_{1905} - R_{1840})/(R_{1905} - R_{1875})$ for nonlinear, demonstrate high coefficients of determination for leaf water content (>0.94) using multi-angular reflectance measurements. Published spectral indices exhibit weak relationships with our calibration dataset. The proposed leaf water content indices perform well, with an overall root mean square error of 0.0024 (g/cm^2) and 0.0026 (g/cm^2) for linear and nonlinear indices, respectively, validated by Leaf Optical Properties Experiment, ANGERS, and multi-angular datasets. The $(R_1 - R_2)/(R_1 - R_3)$ bands show promise for leaf water content estimation. Future studies should encompass more plant species and field data.

Keywords: equivalent water thickness; spectral reflectance variability from various angles; optical remote sensing; viewing angle robust spectral indices

Paper 240116SS received Feb. 19, 2024; revised May 14, 2024; accepted Jul. 4, 2024; published Jul. 26, 2024.

*Address all correspondence to Zhijie Zhang, zhijiezhang@arizona.edu; Qazi Muhammad Yasir, yas984@nenu.edu.cn

1 Introduction

The water content in plant leaves is crucial for photosynthesis and can serve as an indicator of water stress at various growth stages.[1–4] Monitoring leaf water conditions is vital for assessing plant physiological status,[5] detecting drought,[6] predicting wildfires,[7] and other ecological, agricultural, and forestry applications.[8,9] However, traditional methods for obtaining leaf water content data are time-consuming, destructive, and restricted to small study areas, lacking spatial variability information across larger regions.

By analyzing absorption characteristics across different wavelengths, optical methods present a practical approach to assessing the water status of plants.[10–16] Utilizing both theoretical radiative transfer models[17,18] and empirical models,[19,20] researchers can determine leaf water content through spectral reflectance factors. Early investigations established a clear link between leaf and canopy levels.[15,19,21,22] Optical measurements offer diverse means to estimate leaf water content[23–28] facilitating non-destructive monitoring for drought and fire risk assessment.[29–33]

Spectral indices, derived from reflectance factor measurements at specific wavelengths, are predominantly utilized for measuring leaf water content.[31,32,34–36] These indices can be applied across the ground, airborne, and spaceborne scales, offering insights into leaf water content variation with varying levels of accuracy.[23,32,33,35] With advancements in remote sensing technologies, driven by increased spectral and spatial resolution data, the estimation of leaf water content and biochemical parameters has become more precise.[25,35–38] Enhanced geographical coverage and the availability of valuable time series data are facilitated by high-spatial-resolution images captured by aerial or space-based sensors.[25,39,40]

Challenges arise when analyzing leaf or vegetation cover using high spectral and spatial resolution reflectance data. Existing indices for estimating leaf water content are often tailored to specific plant species or measurement conditions.[26,41] Furthermore, in canopy measurements, high-spatial-resolution detectors can distinguish light reflecting from individual leaf components.[39,42] The significance of the multi-angular reflectance factor has been acknowledged in estimating leaf biochemical properties, owing to the variable positions of leaves and diverse illuminating angles.[43–45] The distribution pattern and extent of directional reflectance are influenced by leaf surface specular reflection, which is unrelated to leaf biochemistry.[46–49] However, the impact of multi-angular reflectance on estimating leaf water content is commonly overlooked, as most leaf reflectance measurements are conducted from a single angle, using leaf clips, or integrating spheres.[15,26,34,41] In addition, the anisotropic reflectance of vegetation cover can alter spectral index values due to view-illumination effects,[50,51] posing challenges for the broader adoption of empirical methods. Further exploration into hyperspectral reflection at various viewing angles is necessary to enhance the accuracy of high spectral bandwidth and spatial resolution in predicting leaf water content for ecological, agricultural, and forestry applications.

This study conducted laboratory measurements of multi-angular spectral reflectance factors using leaf samples collected from 10 different plant species. The objective was to introduce a novel spectral index for estimating leaf water content, focusing specifically on equivalent water thickness (EWT). The proposed index was designed to establish a consistent correlation with EWT across varying illumination and viewing angles, enabling precise estimation of EWT from diverse datasets. This angle-independent index provides a convenient and non-destructive approach for accurately determining leaf water content, facilitating rapid assessment of EWT.

2 Material and Methodology

2.1 Reflectance Measurements from Various Leaf Viewing Angles

We measured the multi-angular reflectance parameters of leaves in the lab from April to October, when leaves were in their full growth phase. Our dataset comprised 256 leaf samples from 10 different species (Fig. 1). The samples were collected at Northeast Normal University, Changchun, Jilin Province, China (Table 1). To ensure accuracy, we only selected fresh leaves with a consistent color with no obvious signs of illness.[52,53] We randomly collected leaves at different stages of growth, including young, mature, and senescent leaves, representing a wide range of EWT (Table 1). Leaves undergoing senescence and aging show resemblances to those from plants exposed to diverse stressors such as pollutants, extreme temperatures, drought, and diseases. As a result, our leaf samples represent a broad spectrum of growth conditions.[52] Due to

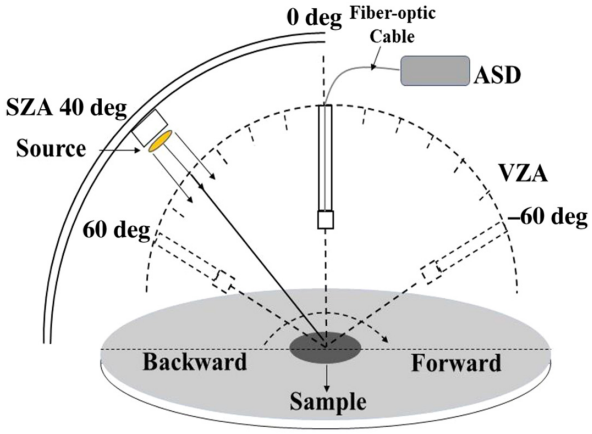

Fig. 1 Primary plane measurement system in the lab. The sun and VZAs are represented by SZA and VZA, respectively.

Table 1 Samples with varying measurement geometries and EWT statistics. The calibration data were used to derive the links between spectral indices and EWT ($n = 256$).

Species	Measurement condition	Sample number	SZA (30 deg)	SZA (40 deg)	VZA (deg)	Mean	Mini	Maxi
Prunus padus L.	Laboratory	23	—	23	−60 to 60	0.0078	0.0059	0.0097
Swida alba Opiz	Laboratory	20	—	20	−60 to 60	0.0090	0.0068	0.0122
Acer saccharum Marsh	Laboratory	20	—	20	−60 to 60	0.0077	0.0054	0.0094
Armeniaca vulgaris Lam.	Laboratory	22	—	22	−60 to 60	0.0106	0.0077	0.0150
Populus L.	Laboratory	20	—	20	−60 to 60	0.0101	0.0065	0.0149
Epipremnum aureum	Laboratory	24	—	24	−60 to 60	0.0248	0.0184	0.0293
Schefflera microphylla Merr.	Laboratory	57	36	21	−60 to 60	0.0319	0.0161	0.0433
Pachira aquatica	Laboratory	41	41		−60 to 60	0.0113	0.0077	0.0152
Juglans	Laboratory	13	—	13	−60 to 60	0.0088	0.0070	0.0103
Citrus limon (L.) Burm. f.	Laboratory	16	16		−60 to 60	0.0147	0.0095	0.0189
Total		256						

variations in leaf surface structures among different species, the reflection patterns under different incident or observational angles may vary. Leaf reflectance characteristics were assessed from various angles in a controlled laboratory setting (Fig. 1).

After harvesting, leaves were placed in sealed plastic bags, along with moist paper towels, to maintain moisture during transportation. To detect spectrum reflection, we utilized the Northeast Normal University Laboratory Goniospectrometer System (NENULGS), as described by Refs. 4, 54, and 55. *NENULGS* incorporates a source of artificial light, an Analytical Spectral Devices FieldSpec 4, and a goniometer. It offers the capacity to measure reflection spectra over a broad range of directions within its hemisphere, capturing wavelengths from 350 to 2500 nm. NENULGS has been extensively applied in studies examining the optical features of leaves.[56–58]

Leaf measurements were undertaken in the principal plane to explore how varying combinations of incident angles and viewing zenith angles (VZAs) impact the estimation. Three incidence zenith angles (30, 40, and 50 deg) and VZAs from −60 to 60 deg with a 10-deg gap were covered by the measurements (Fig. 1). Due to the NENULGS apparatus' constraints, measurements were not possible when the incident and viewing angles coincided in the direction of backward scattering since the least measured phase angle was 8 deg. To calculate reflectance

factors, we obtained measurements at 12 VZAs, where measurements marked with "–" were associated with forward, whereas the others were associated with backward directions.

The leaf sample was placed on an object stage covered with black tape during the measurements. The black background had a reflectance factor smaller than 0.05, ensuring that it had a minimal impact on the leaf reflection and eliminating background effects. The bidirectional reflectance factor (BRF) was calculated as the ratio of the reflected radiance (dLSample) from the leaf sample surface to the reflected radiance (dLReference) from the reference surface (a Spectralon) under the same viewing geometry. This calculation followed the definition provided by[59]

$$\mathrm{BRF}(\lambda,\theta_s,\theta_v,\varphi_s,\varphi_v)=\frac{\mathrm{dL_{Sample}}(\lambda,\theta_s,\theta_v;\varphi_s,\varphi_v)}{\mathrm{dL_{Reference}}(\lambda,\theta_s,\theta_v;\varphi_s,\varphi_v)}\rho_\lambda. \tag{1}$$

The variables θ_s (solar zenith angle of irradiance), θ_v (VZAs), φ_s (incident azimuth angle), φ_v (viewing azimuth angle), and λ (wavelength) were considered in our study. The reflectance factor ρ_λ ranged from 0.9284 to 0.9954.

Further consideration was given to the Leaf Optical Properties Experiment (LOPEX), ANGERS, and multi-angular datasets for the validation of the indices suggested in this work to examine the reliability and generalization of the proposed indices.[31,55]

A ViewSpec software from the analytical spectral device (ASD) manufacturer to resolve the discontinuity problem at 1000 nm attributed to constraints in the ASD spectrometer's configuration.[60,61] In addition, to accomplish spectrum smoothing over the 400- to 2500-nm range, we utilized a Savitzky–Golay polynomial least-square algorithm with a second-order and 20-nm bandwidth window.[62]

2.2 Measurement of Biochemical Properties

Leaf water status can be assessed using various methods, among them is EWT. In this study, EWT was utilized to evaluate the leaf water status. EWT refers to the amount of water content closely associated with the absorption of energy per unit leaf area.[63] The equation for EWT is mentioned as

$$\mathrm{EWT}\ (\mathrm{g/cm^2})=(W_F-W_D)/\mathrm{LA}, \tag{2}$$

where W_F denotes the fresh weight (grams), which was measured within 20 min after clipping, and W_D represents the dry weight (grams), obtained by drying at 80°C for 36 h. LA stands for the leaf area (square centimeter). The statistics for the leaves, which were collected at various stages of growth that produce a wide range of EWT values, are presented in Table 1.

2.3 Validation Datasets from Different Sources

Validation of the algorithm, based on correlations between spectral indices and EWT derived from multi-angle reflectance measurements, utilized three distinct datasets (refer to Table 2). These datasets encompassed a range of developmental stages, leaf surface characteristics, and diverse measurement techniques, including integrating spheres, leaf clips, and multi-angle measurements.

Table 2 Datasets for validation that were utilized in this work to estimate EWT. Table 3 demonstrates an extensive overview of the multi-angle dataset.

	LOPEX	ANGERS	Multi-angle
Spectrophotometer	*Perkin Elmer Lambda 19*	*ASD FieldSpec*	*ASD FieldSpec 4*
Measurement	Laboratory	Laboratory	Laboratory
Spectral range (nm)	400 to 2500	350 to 2500	400 to 250
Number of samples	45	43	78
Reference	64	65	

Table 3 Multi-angle dataset comprises measurements of 78 samples from seven plant species. This dataset was used to construct connections between spectral indices and water indicators.

Species	Measurement condition	Sample number	SZA (40 deg)	SZA (50 deg)	VZA (deg)
Syzygium aromaticum	Laboratory	9			−60 to 60
Pachira aquatica	Laboratory	4			−60 to 60
Juglans	Laboratory	4			−60 to 60
Epipremnum aureum	Laboratory	11	7	4	−60 to 60
Swida alba Opiz	Laboratory	17	17		−60 to 60
Acer saccharum Marsh	Laboratory	25	13	12	−60 to 60
Populus L.	Laboratory	8	8		−60 to 60
Total		78			

The LOPEX, conducted by the European Commission's Joint Research Center, comprised 330 leaf samples from 45 plant species.[66] The ANGERS dataset, from an experiment conducted at National Institute for Agriculture Research in Angers, France, in June 2003, included reflectance and transmittance measurements from 275 leaf samples representing 43 plant species, alongside corresponding biochemical and physical measurements.[64]

The multi-angle dataset, compiled in Changchun, China, in 2020, consisted of 163 leaf samples from 10 plant species, measured in the principal plane. In addition, measurements were conducted on 78 leaves from seven other plant species at random, with further details provided in Table 3.

These datasets, acquired using integrating spheres, leaf clips, and goniometers with spectrometers, encompassed woody and herbaceous species in controlled laboratory conditions. The inclusion of diverse leaf internal and surface structures, EWTs, and optical properties in this study underscores its robustness and applicability. The diversity of plant species and their various growth stages renders this method suitable for evaluating the capability to estimate EWT using both established and newly developed spectral indices.[4,55]

2.4 Spectral Indices for Estimating EWT

In this study, a comprehensive analysis was undertaken using a range of published spectral indices, namely, simple difference, simple ratio, normalized difference, and difference ratio (DR), as outlined in Table 4. These indices have been previously recognized as highly effective in estimating EWT and various other forms of leaf water content across diverse plant species. Importantly, some indices were observed to exhibit minimal sensitivity to variations in leaf surface structure, further highlighting their suitability for accurate EWT estimation.

Ref. 69 employed two DR indices, specifically $(R_{850}-R_{2218})/(R_{850}-R_{1928})$ and $(R_{850}-R_{1788})/(R_{850}-R_{1928})$, for estimating EWT in a limited number of Eucalyptus species. In addition, a VZA was incorporated to diminish specular reflection from leaf surfaces. More recently, DR indices have been demonstrated to be effective in reducing the impact of specular reflection on leaf chlorophyll content estimation[56] and multi-angular reflectance factor.[70] Here, we proposed new DR indices based on laboratory-measured BRF to account for the spectral reflectance impact in the 400- to 2500-nm range. The new index is a ratio of reflectance factors at three specific wavelengths, with one representing specular light reflection from leaves [$\lambda 1$ in Eqs. (3) and (4)]. The denominator utilizes a wavelength that is sensitive to EWT, and the numerator employs a wavelength that is insensitive to EWT.[36] After analyzing reflectance–EWT relationships, the linear index utilized 1905, 1840, and 1875 nm [Eq. (3)]. The nonlinear index used 1845, 1880, and 1910 nm [Eq. (4)]

$$DR=(R_{\lambda 1}-R_{\lambda 2})/(R_{\lambda 1}-R_{\lambda 3})=(R_{1905}-R_{1840})/(R_{1905}-R_{1875}), \tag{3}$$

Table 4 Spectral indices utilized to estimate EWT.

Index	Formula	References
Normalized differential water index (NDWI)	$(R_{860} - R_{1240})/(R_{860} + R_{1240})$	67
Normalized differential water index (NDWI)	$(R_{860} - R_{1640})/(R_{860} + R_{1640})$	66
	$(R_{850} - R_{2218})/(R_{850} - R_{1928})$	68
	$(R_{850} - R_{1788})/(R_{850} - R_{1928})$	68
Moisture stress index (MSI)	R_{1600}/R_{820}	13
Simple ratio water index (SRWI)	R_{860}/R_{1240}	46
Normalized difference water index centered at 1640 nm ($NDWI_{1640}$)	$(R_{858} - R_{1640})/(R_{858} + R_{1640})$	66
Normalized difference water index centered at 2130 nm ($NDWI_{2130}$)	$(R_{858} - R_{2130})/(R_{858} + R_{2130})$	66
Difference ratio (linear)	$(R_{1905} - R_{1840})/(R_{1905} - R_{1875})$	Proposed in this study
Difference ratio (nonlinear)	$(R_{1845} - R_{1880})/(R_{1845} - R_{1910})$	Proposed in this study

$$DR = (R_{\lambda 1} - R_{\lambda 2})/(R_{\lambda 1} - R_{\lambda 3}) = (R_{1845} - R_{1880})/(R_{1845} - R_{1910}). \quad (4)$$

For selecting the three wavelengths in the DR index, it is essential to eliminate wavelength-independent specular reflection from the leaf surface. Deep absorption bands, often found in blue and red wavelengths, are typically chosen as representative of the specular reflection of leaves.[36] Specular reflection wavelengths must also have constant reflection values and be unaffected by variations in EWT. This ensures their suitability and reliability in spectral index calculations for EWT estimation.

This study aimed to identify wavelengths within the 400- to 2500-nm range that are capable of effectively removing specular reflection that originates from the surface of the leaf. Each wavelength in the range was tested for its suitability in achieving this goal. During the selection process, the reflectance factor at each wavelength in the 400- to 2500-nm spectrum was subtracted from the reflectance at another wavelength within the same range. The obtained subtracted reflectance factor was subsequently correlated with EWT to identify the wavelengths that are most relevant for estimating leaf water content. As specular reflection does not relate to the leaf's EWT, we expected the R^2 values ($R^2_{\text{reduce specular reflection}}$) at each wavelength to increase compared with the original R^2 values (R^2_{original}) obtained without accounting for specular reflection. Subsequently, the cumulative rise in R^2 across the entire 400- to 2500-nm range was evaluated to gauge the influence of specular reflection from the leaf surface. Equation (5) defines the cumulated R^2 increase as follows:

$$\text{cumulated } R^2 \text{ increase} = (R^2_{\text{reduce specular reflection}} - R^2_{\text{original}}). \quad (5)$$

A suitable wavelength for eliminating specular reflection from the leaf surface is expected to exhibit a higher cumulative R^2 increase across the 400- to 2500-nm range than other wavelengths. Our wavelength optimization method differs from previous studies[36,68] as we account for the removal of specular reflection from the leaf surface effect. By reducing specular effects, our approach enables more accurate estimations of leaf biochemical parameters, particularly EWT.

3 Results

3.1 Leaf Reflection Factors: Spectral Features and Distribution

Spectral reflectance factors at various EWTs for the nadir VZA are depicted in Fig. 2, alongside laboratory-measured BRFs. An increase in EWT results in a noticeable decrease in reflectance,

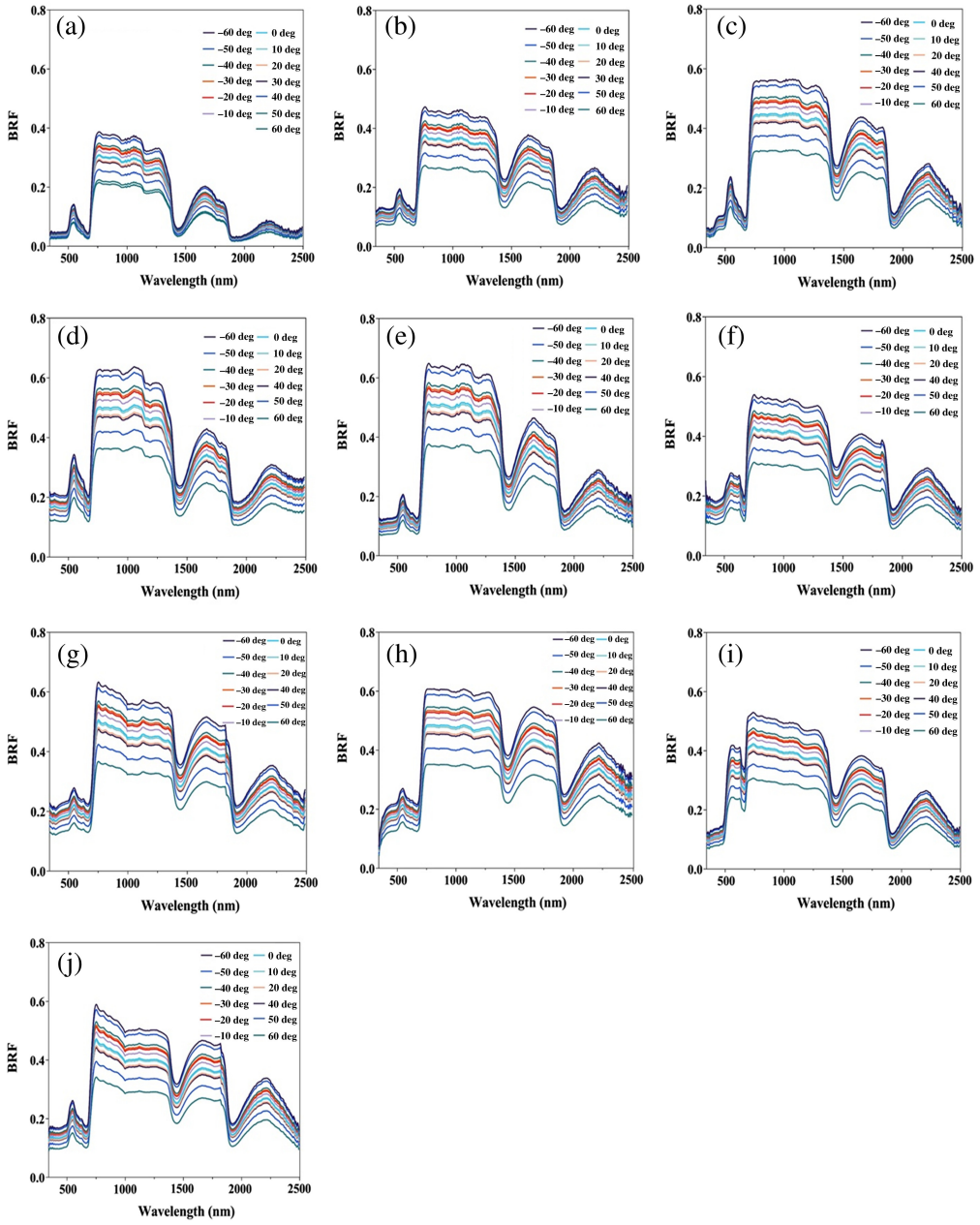

Fig. 2 Leaves BRF at nadir direction with variable EWT. (a) *Schefflera microphylla* Merr. (b) *Pachira aquatica*. (c) *Juglans*. (d) *Epipremnum aureum*. (e) *Citrus limon* (L.) Burm. f. (f) *Prunus padus* L. (g) *Armeniaca vulgaris* Lam. (h) *Populus* L. (i) *Acer saccharum* Marsh. (j) *Swida alba* Opiz.

particularly in the near-infrared and shortwave infrared wavelengths, particularly above 1300 nm, due to significant leaf water absorption (Fig. 2). These spectral characteristics lay the groundwork for estimating EWT using spectral indices. In addition, analyzing the distribution of multi-angular reflectance factors aids in understanding leaf reflection properties across different species.

Moreover, Fig. 3 illustrates the BRFs acquired from 10 plant species at seven different wavelengths. The figure highlights distinct angular distributions observed among the various species, strategically positioned at prominent peaks and valleys within the reflection spectra. While this study did not include an analysis of leaf surface structure, the diverse distribution of BRFs suggests variations in surface properties across plant species. By establishing a reliable spectral index applicable across diverse plant species, the study aims to ensure accurate estimates of

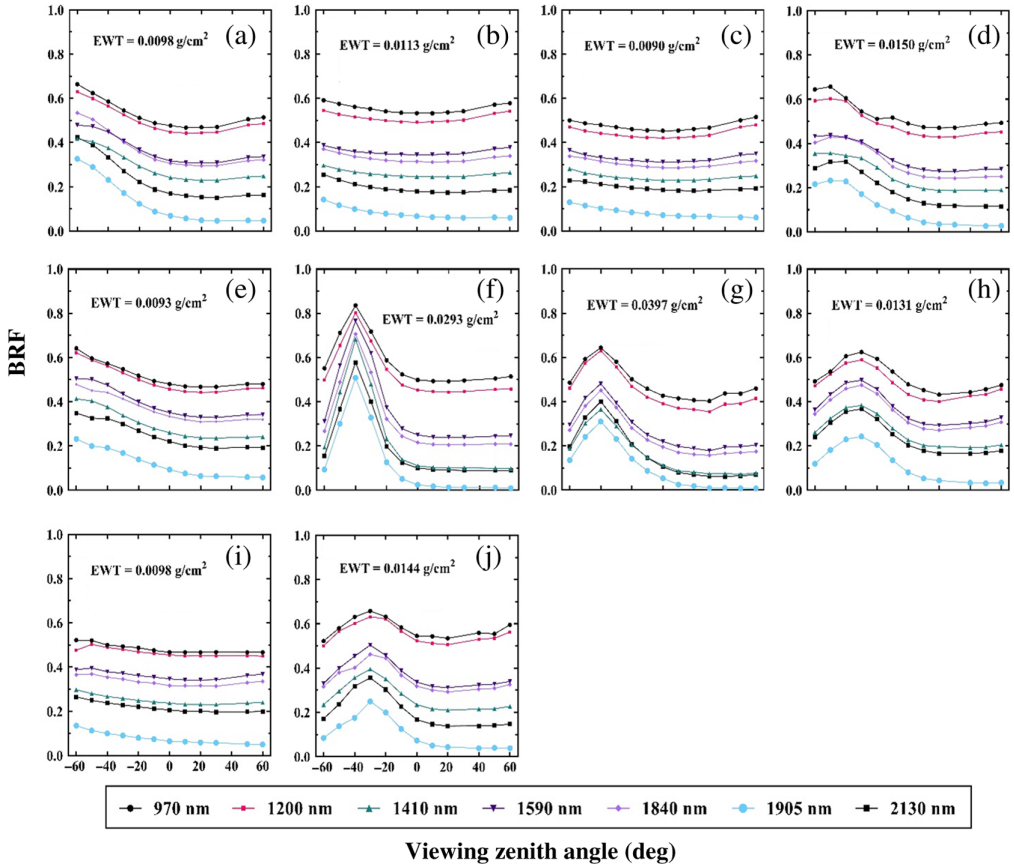

Fig. 3 In laboratory measurements, the BRF of leaves was distributed angularly. "–" denotes forward. The chosen wavelengths were typically used to describe regular reflectance factor peaks and valleys in the electromagnetic spectrum (350 to 2500 nm). (a) *Prunus padus* L. (b) *Swida alba* Opiz. (c) *Acer saccharum* Marsh. (d) *Armeniaca vulgaris* Lam. (e) *Populus* L. (f) *Epipremnum aureum*. (g) *Schefflera microphylla* Merr. (h) *Pachira aquatica*. (i) *Juglans*. (j) *Citus limon* (L.) Burn. f.

EWT. Utilizing multi-angular reflectance factors with varying values and distribution patterns, the effectiveness of existing spectral indices for EWT estimation was evaluated.

3.2 Lab-Measured Multi-angular Reflectance for Examining Spectral Indices and EWT

In the lab-measured multi-angular reflectance analysis to examine spectral indices and EWT, Fig. 4 illustrates the relationships between the examined spectral indices (measured using BRF) and EWT for leaves with recorded VZAs. Among the eight existing spectral indices, weak relationships with EWT were observed, particularly influenced by viewing angles in forward scattering directions. Specifically, R^2 values for most spectral indices decreased at −30, −40, or −50 deg VZAs, with a slight increase at −60 deg. Conversely, near the nadir and in backward scattering directions, the existing spectral indices displayed relatively high R^2 values with a weak dependence on VZAs.

The results suggest that the recently suggested DR indices, $(R_{1905} - R_{1840})/(R_{1905} - R_{1875})$ and $(R_{1845} - R_{1880})/(R_{1845} - R_{1910})$, exhibit a strong connection with EWT and are not influenced by VZAs, as indicated by the laboratory measurements of multi-angular reflectance factors (BRF). The R^2 values for each spectral index, obtained by combining spectral measurements across all VZAs and including data from the principal plane (Table 1), are shown in the right column of Fig. 4. The proposed DR indices exhibit the strongest relationship with EWT, with an R^2 value of 0.95. On the other hand, other indices show weaker relationships with EWT when all multi-angular reflectance factors are considered, mainly due to weak connections in the forward scattering direction or different slopes of the formula at each VZA. The study suggests

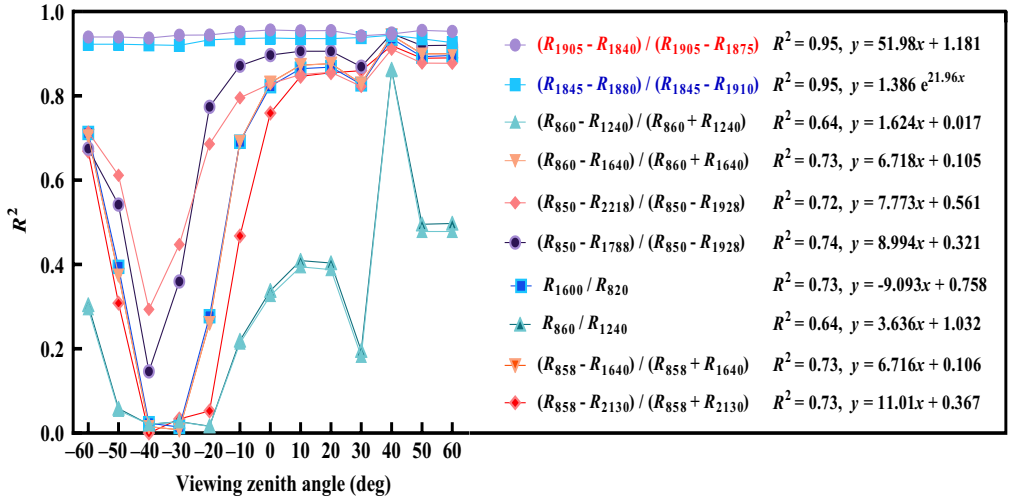

Fig. 4 Depicts spectral index–EWT relationships for all calibration samples at various VZAs. Laboratory-measured multi-angular BRFs were used. The right column displays R^2 values and equations derived from the spectral index–EWT relationship across all viewing directions ($n = 256$).

limitations in applying previously published spectral indices to samples with reflectance factors from different VZAs. The proposed DR indices stand out with a high R^2 value and consistent slopes at each VZA. Furthermore, the consistent performance of the proposed DR indices across all laboratory samples indicates their robustness.

3.3 EWT Estimation from Validation Dataset

To assess the predictability of the newly proposed DR indices, which exhibited the strongest relationship with leaf EWT, three datasets were utilized. These datasets comprised measurements taken from both single angles and multi-angles, as detailed in Tables 2 and 3. Furthermore, the performance of all eight existing spectral indices was compared with the proposed DR indices. The calibration dataset (the rightmost column in Fig. 4) was used to develop algorithms for each spectral index, considering reflectance factors of leaf samples from all samples and VZAs. Table 5 demonstrates the root mean square error (RMSE) values for the eight spectral indices across each database.

Table 5 RMSE values for the eight spectral indices calculated in the validation dataset. Estimated EWT was determined using algorithms (Fig. 4) developed based on calibration data and spectral index. The combined results from the validation datasets are presented in the last column.

Indices	LOPEX	ANGERS	Multi-angle	Combined
(1)	0.0026	0.0024	0.0041	0.0041
(2)	0.0037	0.0032	0.0059	0.0060
(3)	0.0049	0.0043	0.0049	0.0053
(4)	0.0053	0.0059	0.0057	0.0064
(5)	0.0061	0.0062	0.0061	0.0071
(6)	0.0026	0.0028	0.0063	0.0051
(7)	0.0039	0.0034	0.0072	0.0079
(8)	0.0057	0.0053	0.0046	0.0051
Proposed DR linear index	0.0019	0.0015	0.0021	0.0024
Proposed DR nonlinear index	0.0018	0.0015	0.0023	0.0026

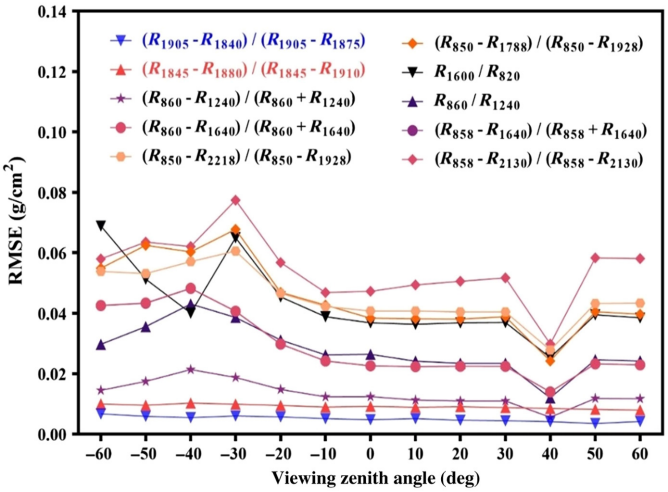

Fig. 5 RMSE of eight spectral and the proposed EWT indices in the principal plane for all validation samples at VZAs (13 directions). The blue and red indices in the left column (top two) represent linear and nonlinear indices, respectively.

After consolidating all validation datasets, we observed that the algorithm based on the proposed DR indices (Fig. 4, top right) demonstrated the highest estimation accuracy, yielding the lowest RMSE when combining all three validation databases, specifically RMSE $=$ $0.0024\ (\mathrm{g/cm^2})$ and $0.0026\ (\mathrm{g/cm^2})$. As indicated in Table 5, the proposed DR indices emerged as the most effective for estimating EWT. Furthermore, our findings revealed that these DR indices not only exhibited insensitivity to VZAs within the principal plane but also demonstrated independence from directions outside the principal plane, thus providing precise estimations of EWT in the multi-angle dataset (Fig. 5). These results suggest that the algorithm derived from the proposed DR indices is accurate and consistent in estimating EWT across diverse plant species with varying leaf structures under different measurement conditions

4 Discussion

4.1 Stability of the Indices for Defining Leaf Water Status

The proposed EWT linear index, calculated as $(R_{1905} - R_{1840})/(R_{1905} - R_{1875})$, and EWT nonlinear index, calculated as $(R_{1845} - R_{1880})/(R_{1845} - R_{1910})$, were thoroughly tested using various odd combinations within the calibration dataset, covering wavelengths up to 61 nm in both forward and backward directions. A total of 29 combinations of the proposed indices were generated, with increments of odd numbers (5, 7, 9, 11, 13, and so on, up to 61 nm) to obtain an average.

These combinations demonstrated stability and a strong determination coefficient, validating their accuracy and reliability, as illustrated in Figs. 6 and 7. The same testing process was adopted by Ref. 71 to assess how the proposed index responds to different wavelength combinations. For the nonlinear index, a similar methodology was employed, and the changes in wavelength ($\Delta\lambda$) at the corresponding regions of the proposed index were represented in Figs. 6 and 7. The results indicate that the proposed EWT linear and nonlinear indices are robust and dependable for the intended purpose.

4.2 Correlation Coefficients of the Individual Wavelength of the Proposed Indices

The optical properties of leaves underwent changes, characterized by a gradual increase in relative reflectance at different wavelengths. However, several published studies presented conflicting findings regarding leaf reflectance alterations, with some showing irregularities, an overall increase in leaf reflectivity,[72,73] a decrease,[74] and others reporting no significant changes in reflectance.[28,75]

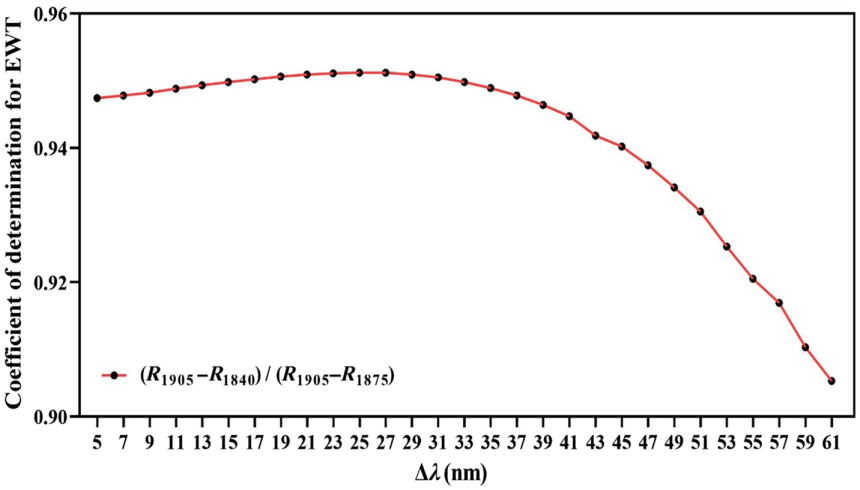

Fig. 6 Stability of the proposed bandwidth in the linear index $(R_{1905} - R_{1840})/(R_{1905} - R_{1875})$ of EWT.

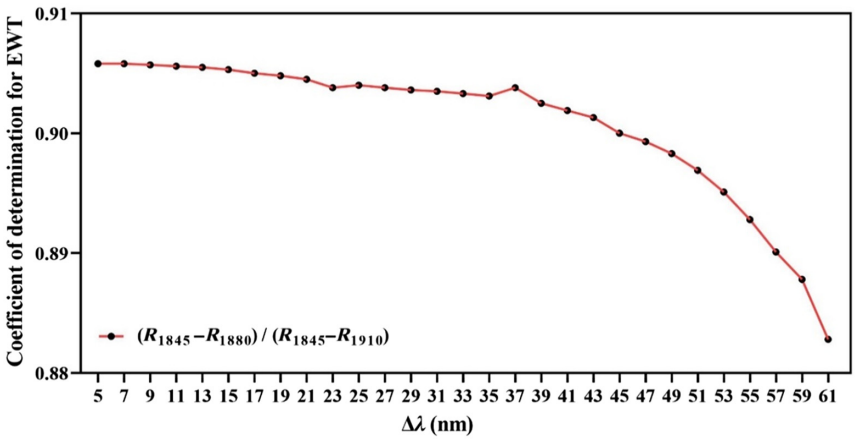

Fig. 7 Stability of the proposed bandwidth index for linear nonlinear $(R_{1845} - R_{1880})/(R_{1845} - R_{1910})$ of EWT.

To address this variability, we adopted a meticulous approach, which involved carefully defining each band of the indices and examining their relationship with reflectance, as depicted in Fig. 8. This method allowed us to gain deeper insights into the impact of the indices on leaf reflectance and provided a more comprehensive understanding of the observed changes in optical properties.

4.3 Importance of Understanding Multi-angle Leaf Reflectance Variables

The distribution of leaf reflectance factors, influenced by specular reflection from the leaf surface, exhibits significant anisotropy, particularly in forward directions within the principal plane. This anisotropy has a pronounced effect on the BRF of leaves, particularly those with prominent specular reflections. Previous studies have consistently shown that leaf structure tends to result in lower reflectance in forward directions.[51,61,76,77]

At moderate or low remote sensing resolutions, averaging leaf reflectance factors across different directions can mitigate the impact of specular effects on leaf water content (EWT) estimation. However, for high spatial resolution data, considering multi-angular leaf reflection becomes imperative.[21,42,47,78] With advancements in technology, it is now feasible to obtain high spatial resolution data for small leaf sections,[79] allowing for the measurement of reflected light from various viewing directions.[21,42,47,78]

Specular reflection from the leaf surface influences the distribution and intensity of multi-angular reflectance factors, although it does not directly correlate with the leaf's biochemical

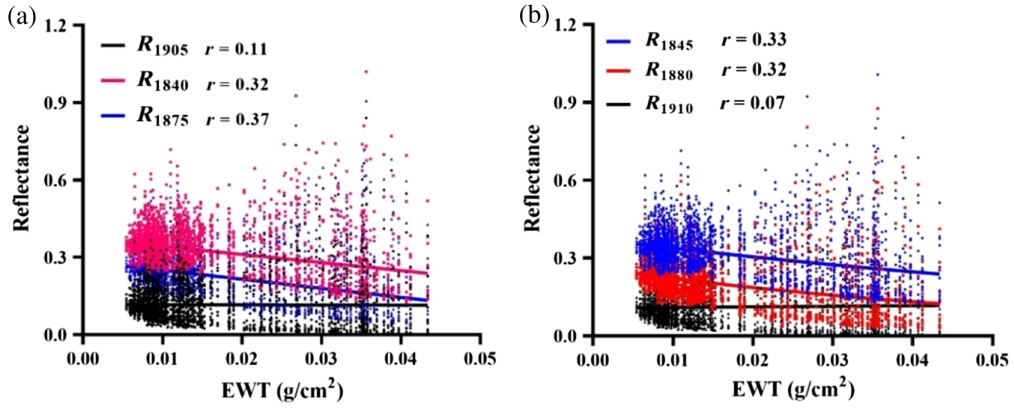

Fig. 8 Relationship between EWT and reflectance from calibration data set at (a) linear (bands): R_{1905}, R_{1840}, and R_{1875} (nm) and (b) nonlinear (bands): R_{1845}, R_{1880}, and R_{1910} (nm). The graphs indicate the correlation coefficients (r).

properties. Nevertheless, individual leaf-level spectroscopic studies contribute to our understanding of plant-radiation interactions, which can be extrapolated to the canopy level.[80–83] Therefore, conducting comprehensive studies to examine the correlations between EWT and spectral indices, using multi-angular reflectance factors from diverse plant species in laboratory settings, holds significant importance for remote sensing experts.

Distinct patterns of reflectance factors in leaves from different plant species, as illustrated in Fig. 3, are largely attributed to variations in leaf surface features, which differ between species or developmental stages and affect the occurrence of specular reflection from the leaf surface.[46,84] Specular reflection primarily occurs in the forward direction and, to a lesser extent, in the backward or nadir directions. Consequently, weak specular reflection in nadir directions minimally affects the relationships between most spectral indices and EWT (Fig. 4).

Conversely, when specular reflection dominates the overall reflection, particularly in forward scattering directions (Fig. 3), the associations between spectral indices and EWT weaken (Fig. 4), resulting in diminished accuracy in EWT estimation. The accuracy of estimation typically deteriorates in practical applications when data from a single pixel are predominantly affected by specular reflection from the leaf surface. Therefore, there is a need for a viewing angle-independent spectral index with an effective relationship to EWT for remote sensing applications across various fields.

4.4 Strengths and Limitations of the Proposed Indices

Existing EWT estimation spectral indices are primarily based on leaf reflectance or reflectance factors, measured through integrating spheres, spectrometers with leaf clips, or spectrometers in the nadir direction. These approaches have been employed in previous studies by researchers such as Refs. 13, 26, and 85. However, specular reflection from the leaf surface in these measurement directions has not been extensively addressed by scholars who are working on EWT estimation. Although this form of reflection has little impact on spectral measurements, taking it into account is essential for increasing the reliability of EWT measurement.

The newly proposed DR indices offer significant advancements in minimizing the impact of specular reflection from the leaf surface across diverse plant species and illumination-viewing geometries, resulting in a stronger correlation with EWT than other existing indices investigated in this research. Moreover, the DR indices demonstrate no sensitivity to multi-angular reflectance factors, thereby enhancing their accuracy and robustness for EWT estimation. Their reduced sensitivity to viewing angles makes them reliable and applicable across various environmental conditions, making the DR indices a promising choice for EWT estimation.

An additional advantage is their applicability to diverse measured and simulated datasets, covering various plant species and regions. This adaptability is attributed to the multi-angular reflectance factors, which incorporate reflection values similar to leaf clip or integrating sphere measurements while considering the influence of specular reflection from the leaf surface. These DR indices are versatile, facilitating EWT estimation using hyperspectral data and sensor design.

While the individual wavelength was not specifically validated in this study, we are confident in accurate EWT predictions with sensors having the same wavelength as the ASD (ranging from 3 nm in the 400- to 1000-nm region to 6 nm in the 1000- to 2500 nm region). The wide-ranging applicability of the proposed DR indices makes them suitable for diverse datasets and settings, holding promise for accurate EWT estimation and sensor design in future applications.

The indices have the potential for reducing specular reflection and reliably estimating EWT across viewing angles. However, it is vital to recognize limitations, such as restricted species representation, variances between lab and field conditions, and the influence of spectral band choice and instrument sensitivity. Addressing these through broader species inclusion, field validations, and sensitivity analyses would bolster the robustness and practicality of our method.

5 Conclusion

In this study, we introduced two novel DR indices, namely, $(R_{1905} - R_{1840})/(R_{1905} - R_{1875})$ for linear measurements and $(R_{1845} - R_{1880})/(R_{1845} - R_{1910})$ for nonlinear measurements. These DR indices present a double advantage: they efficiently reduce the impact of specular reflection from the leaf surface, and they furnish precise EWT estimations for multi-angular measurements. Furthermore, a theoretical rationale for the selection of specific wavelengths in the DR indices. The chosen wavelengths were carefully considered to optimize the reduction of specular reflection while retaining essential spectral information relevant to EWT estimation. By combining these innovative DR indices with the theoretical justification for wavelength selection, this study presents a valuable contribution toward improving the accuracy and reliability of EWT estimation in diverse measurement scenarios, making it a promising development in the field of plant spectral analysis.

Furthermore, we conducted a comprehensive validation of both existing spectral indices and the newly proposed indices for EWT estimation. This validation involved using multi-angular reflectance factors from 10 diverse plant species in a controlled laboratory environment. Our findings revealed that existing spectral indices exhibited a satisfactory correlation with EWT in nadir and backward directions. However, their correlation was notably lower in forward directions, indicating the influence of specular reflection from leaf surfaces. In contrast, the newly proposed indices effectively mitigated the impact of specular reflection, resulting in more consistent and reliable EWT estimations across varying viewing angles. This underscores the importance of considering specular reflection in multi-angular measurements and highlights the superiority of our proposed indices. These insights contribute to our understanding of factors influencing spectral indices' performance in EWT estimation and offer valuable guidance for future research and applications in plant spectral analysis.

The proposed indices demonstrate stable and robust relationships with EWT across all viewing angles. The algorithm based on multi-angular reflectance factors enables accurate EWT estimation across various datasets without the need for re-parameterization for each plant species. This generic algorithm streamlines EWT estimation from reflection measurements, offering a reliable and practical approach applicable to measurements from any angle. Thus, our approach provides an efficient and accurate method for calculating EWT across a range of plant species, with potential applications in forestry and botanical studies

Code and Data Availability

Data will be provided upon request.

Acknowledgments

This study was jointly financed by the Major Science and Technology Program of Ministry of Water Resources (Grant No. SKS-2022008) and the project of "Construction of a distributed non-point source pollution model" in the Hulunbuir City basin (Grant No. E2C20529), Karst Plateau Resources and Environmental Remote Sensing Talent Team [Grant No. BWRLT (2023) No. 14], and Intelligent Geographic Spatial Information Application Engineering Center [Grant No. BKLH (2023) No. 08]. We extend our warmest thanks to all individuals involved in the submission of this paper for their contributions toward the successful publication of the present work.

References

1. J. Galmés, H. Medrano, and J. Flexas, "Photosynthetic limitations in response to water stress and recovery in Mediterranean plants with different growth forms," *New Phytol.* **175**(1), 81–93 (2007).
2. Y. Osakabe et al., "Response of plants to water stress," *Front. Plant Sci.* **5**, 86 (2014).
3. N. Smirnoff, "Tansley review no. 52. The role of active oxygen in the response of plants to water deficit and desiccation," *New Phytol.* **125**(1), 27–58 (1993).
4. X. Li et al., "A multi-angular invariant spectral index for the estimation of leaf water content across a wide range of plant species in different growth stages," *Remote Sens. Environ.* **253**, 112230 (2021).
5. E. Garnier and G. Laurent, "Leaf anatomy, specific mass and water content in congeneric annual and perennial grass species," *New Phytol.* **128**(4), 725–736 (1994).
6. P. Nautiyal, N. R. Rachaputi, and Y. Joshi, "Moisture-deficit-induced changes in leaf-water content, leaf carbon exchange rate and biomass production in groundnut cultivars differing in specific leaf area," *Field Crops Res.* **74**(1), 67–79 (2002).
7. D. Viegas, M. Viegas, and A. Ferreira, "Moisture content of fine forest fuels and fire occurrence in central Portugal," *Int. J. Wildland Fire* **2**(2), 69–86 (1992).
8. A. F. Huberty and R. F. Denno, "Plant water stress and its consequences for herbivorous insects: a new synthesis," *Ecology* **85**(5), 1383–1398 (2004).
9. S. W. Ritchie, H. T. Nguyen, and A. S. Holaday, "Leaf water content and gas-exchange parameters of two wheat genotypes differing in drought resistance," *Crop Sci.* **30**(1), 105–111 (1990).
10. P. Ceccato et al., "Detecting vegetation leaf water content using reflectance in the optical domain," *Remote Sens. Environ.* **77**(1), 22–33 (2001).
11. F. M. Danson and P. Bowyer, "Estimating live fuel moisture content from remotely sensed reflectance," *Remote Sens. Environ.* **92**(3), 309–321 (2004).
12. H. Gausman and W. Allen, "Optical parameters of leaves of 30 plant species," *Plant Physiol.* **52**(1), 57–62 (1973).
13. E. R. Hunt, Jr. and B. N. Rock, "Detection of changes in leaf water content using near-and middle-infrared reflectances," *Remote Sens. Environ.* **30**(1), 43–54 (1989).
14. R. E. Martin et al., "Remote measurement of canopy water content in giant sequoias (Sequoiadendron giganteum) during drought," *Forest Ecol. Manage.* **419**, 279–290 (2018).
15. J. Peñuelas et al., "Reflectance indices associated with physiological changes in nitrogen-and water-limited sunflower leaves," *Remote Sens. Environ.* **48**(2), 135–146 (1994).
16. C. J. Tucker, "Remote sensing of leaf water content in the near infrared," *Remote Sens. Environ.* **10**(1), 23–32 (1980).
17. S. Jacquemoud and F. Baret, "PROSPECT: a model of leaf optical properties spectra," *Remote Sens. Environ.* **34**(2), 75–91 (1990).
18. S. Jacquemoud et al., "PROSPECT+ SAIL models: a review of use for vegetation characterization," *Remote Sens. Environ.* **113**, S56–S66 (2009).
19. J. Peñuelas et al., "The reflectance at the 950–970 nm region as an indicator of plant water status," *Int. J. Remote Sens.* **14**(10), 1887–1905 (1993).
20. J. Peñuelas and J. Llusià, "Effects of carbon dioxide, water supply, and seasonality on terpene content and emission by Rosmarinus officinalis," *J. Chem. Ecol.* **23**, 979–993 (1997).
21. P. P. Roosjen et al., "Improved estimation of leaf area index and leaf chlorophyll content of a potato crop using multi-angle spectral data–potential of unmanned aerial vehicle imagery," *Int. J. Appl. Earth Observ. Geoinf.* **66**, 14–26 (2018).
22. E. R. Hunt, Jr., B. N. Rock, and P. S. Nobel, "Measurement of leaf relative water content by infrared reflectance," *Remote Sens. Environ.* **22**(3), 429–435 (1987).
23. L. Cotrozzi et al., "Using foliar spectral properties to assess the effects of drought on plant water potential," *Tree Physiol.* **37**(11), 1582–1591 (2017).
24. I. Pôças et al., "Toward a generalized predictive model of grapevine water status in Douro region from hyperspectral data," *Agric. Forest Meteorol.* **280**, 107793 (2020).
25. T. Paz-Kagan et al., "Landscape-scale variation in canopy water content of giant sequoias during drought," *Forest Ecol. Manage.* **419**, 291–304 (2018).
26. O. Vergara-Díaz et al., "Leaf dorsoventrality as a paramount factor determining spectral performance in field-grown wheat under contrasting water regimes," *J. Exp. Botany* **69**(12), 3081–3094 (2018).
27. C. Xu et al., "Monitoring crop water content for corn and soybean fields through data fusion of MODIS and Landsat measurements in Iowa," *Agric. Water Manage.* **227**, 105844 (2020).
28. M. Yebra et al., "A global review of remote sensing of live fuel moisture content for fire danger assessment: moving towards operational products," *Remote Sens. Environ.* **136**, 455–468 (2013).
29. H. C. Claudio et al., "Monitoring drought effects on vegetation water content and fluxes in chaparral with the 970 nm water band index," *Remote Sens. Environ.* **103**(3), 304–311 (2006).

30. F. M. Danson and Y. Aldakheel, "Diurnal water stress in sugar beet: Spectral reflectance measurements and modeling," *Agronomie* **20**(1), 31–39 (2000).
31. S. M. de Jong, E. A. Addink, and J. C. Doelman, "Detecting leaf-water content in Mediterranean trees using high-resolution spectrometry," *Int. J. Appl. Earth Observ. Geoinf.* **27**, 128–136 (2014).
32. T. J. Jackson et al., "Vegetation water content mapping using Landsat data derived normalized difference water index for corn and soybeans," *Remote Sens. Environ.* **92**(4), 475–482 (2004).
33. S. Stagakis et al., "Monitoring water stress and fruit quality in an orange orchard under regulated deficit irrigation using narrow-band structural and physiological remote sensing indices," *ISPRS J. Photogramm. Remote Sens.* **71**, 47–61 (2012).
34. B. Das et al., "Comparison of different uni-and multi-variate techniques for monitoring leaf water status as an indicator of water-deficit stress in wheat through spectroscopy," *Biosyst. Eng.* **160**, 69–83 (2017).
35. Q.-X. Yi et al., "Estimation of leaf water content in cotton by means of hyperspectral indices," *Comput. Electron. Agric.* **90**, 144–151 (2013).
36. D. A. Sims and J. A. Gamon, "Estimation of vegetation water content and photosynthetic tissue area from spectral reflectance: a comparison of indices based on liquid water and chlorophyll absorption features," *Remote Sens. Environ.* **84**(4), 526–537 (2003).
37. Y. Ge et al., "High-throughput analysis of leaf physiological and chemical traits with VIS–NIR–SWIR spectroscopy: a case study with a maize diversity panel," *Plant Methods* **15**(1), 1–12 (2019).
38. L. Zhang et al., "Monitoring the leaf water content and specific leaf weight of cotton (*Gossypium hirsutum* L.) in saline soil using leaf spectral reflectance," *Eur. J. Agron.* **41**, 103–117 (2012).
39. S. Jay et al., "Retrieving LAI, chlorophyll and nitrogen contents in sugar beet crops from multi-angular optical remote sensing: comparison of vegetation indices and PROSAIL inversion for field phenotyping," *Field Crops Res.* **210**, 33–46 (2017).
40. L. Zhang et al., "Mapping maize water stress based on UAV multispectral remote sensing," *Remote Sens.* **11**(6), 605 (2019).
41. M. Kovar et al., "Evaluation of hyperspectral reflectance parameters to assess the leaf water content in soybean," *Water* **11**(3), 443 (2019).
42. S. Hancock, R. Gaulton, and F. M. Danson, "Angular reflectance of leaves with a dual-wavelength terrestrial LiDAR and its implications for leaf-bark separation and leaf moisture estimation," *IEEE Trans. Geosci. Remote Sens.* **55**(6), 3084–3090 (2017).
43. Y. Knyazikhin et al., "Hyperspectral remote sensing of foliar nitrogen content," *Proc. Natl. Acad. Sci.* **110**(3), E185–E192 (2013).
44. X. Pan et al., "A novel exposed coal index combining flat spectral shape and low reflectance," *IEEE Trans. Geosci. Remote Sens.* **61**, 1–16 (2023).
45. Z. Chen et al., "Mapping mangrove using a red-edge mangrove index (REMI) based on Sentinel-2 multispectral images," *IEEE Trans. Geosci. Remote Sens.* **61**, 1–11 (2023).
46. L. Bousquet et al., "Leaf BRDF measurements and model for specular and diffuse components differentiation," *Remote Sens. Environ.* **98**(2-3), 201–211 (2005).
47. S. Jay et al., "Estimating leaf chlorophyll content in sugar beet canopies using millimeter-to centimeter-scale reflectance imagery," *Remote Sens. Environ.* **198**, 173–186 (2017).
48. L. Grant, C. Daughtry, and V. Vanderbilt, "Variations in the polarized leaf reflectance of Sorghum bicolor," *Remote Sens. Environ.* **21**(3), 333–339 (1987).
49. V. Vanderbilt et al., "Specular, diffuse, and polarized light scattered by two wheat canopies," *Appl. Opt.* **24**(15), 2408–2418 (1985).
50. L. S. Galvão et al., "View-illumination effects on hyperspectral vegetation indices in the Amazonian tropical forest," *Int. J. Appl. Earth Observ. Geoinf.* **21**, 291–300 (2013).
51. F. Li et al., "Improving BRDF normalisation for Landsat data using statistical relationships between MODIS BRDF shape and vegetation structure in the Australian continent," *Remote Sens. Environ.* **195**, 275–296 (2017).
52. A. Gitelson and M. N. Merzlyak, "Spectral reflectance changes associated with autumn senescence of *Aesculus hippocastanum* L. and *Acer platanoides* L. leaves. Spectral features and relation to chlorophyll estimation," *J. Plant Physiol.* **143**(3), 286–292 (1994).
53. A. A. Gitelson, Y. Gritz, and M. N. Merzlyak, "Relationships between leaf chlorophyll content and spectral reflectance and algorithms for non-destructive chlorophyll assessment in higher plant leaves," *J. Plant Physiol.* **160**(3), 271–282 (2003).
54. Z. Sun, Z. Wu, and Y. Zhao, "Semi-automatic laboratory goniospectrometer system for performing multi-angular reflectance and polarization measurements for natural surfaces," *Rev. Sci. Instrum.* **85**(1), 014503 (2014).
55. Q. M. Yasir et al., "Spectral indices for tracing leaf water status with hyperspectral reflectance data," *J. Appl. Remote Sens.* **17**(1), 014523 (2023).

56. D. Li et al., "Assessment of unified models for estimating leaf chlorophyll content across directional-hemispherical reflectance and bidirectional reflectance spectra," *Remote Sens. Environ.* **231**, 111240 (2019).
57. Z. Sun et al., "Photopolarimetric properties of leaf and vegetation covers over a wide range of measurement directions," *J. Quant. Spectrosc. Radiat. Transf.* **206**, 273–285 (2018).
58. J. Sun et al., "Wavelength selection of the multispectral lidar system for estimating leaf chlorophyll and water contents through the PROSPECT model," *Agric. Forest Meteorol.* **266**, 43–52 (2019).
59. G. Schaepman-Strub et al., "Reflectance quantities in optical remote sensing—definitions and case studies," *Remote Sens. Environ.* **103**(1), 27–42 (2006).
60. J. Suomalainen et al., "Polarised bidirectional reflectance factor measurements from vegetated land surfaces," *J. Quant. Spectrosc. Radiat. Transf.* **110**(12), 1044–1056 (2009).
61. J. I. Peltoniemi et al., "BRDF measurement of understory vegetation in pine forests: dwarf shrubs, lichen, and moss," *Remote Sens. Environ.* **94**(3), 343–354 (2005).
62. A. Savitzky and M. J. Golay, "Smoothing and differentiation of data by simplified least squares procedures," *Anal. Chem.* **36**(8), 1627–1639 (1964).
63. S. Jacquemoud et al., "Estimating leaf biochemistry using the PROSPECT leaf optical properties model," *Remote Sens. Environ.* **56**(3), 194–202 (1996).
64. J.-B. Feret et al., "PROSPECT-4 and 5: advances in the leaf optical properties model separating photosynthetic pigments," *Remote Sens. Environ.* **112**(6), 3030–3043 (2008).
65. G. Le Maire, C. François, and E. Dufrene, "Towards universal broad leaf chlorophyll indices using PROSPECT simulated database and hyperspectral reflectance measurements," *Remote Sens. Environ.* **89**(1), 1–28 (2004).
66. B. Hosgood et al., "Leaf optical properties experiment 93 (LOPEX93)," Report EUR 16095, 1–46 (1995).
67. B.-C. Gao, "NDWI—a normalized difference water index for remote sensing of vegetation liquid water from space," *Remote Sens. Environ.* **58**(3), 257–266 (1996).
68. B. Datt, "A new reflectance index for remote sensing of chlorophyll content in higher plants: tests using Eucalyptus leaves," *J. Plant Physiol.* **154**(1), 30–36 (1999).
69. B. Datt, "Remote sensing of water content in Eucalyptus leaves," *Aust. J. Botany* **47**(6), 909–923 (1999).
70. W. Li et al., "Estimation of the leaf chlorophyll content using multiangular spectral reflectance factor," *Plant Cell Environ.* **42**(11), 3152–3165 (2019).
71. Z. Cao, Q. Wang, and C. Zheng, "Best hyperspectral indices for tracing leaf water status as determined from leaf dehydration experiments," *Ecol. Indicators* **54**, 96–107 (2015).
72. G. A. Carter, "Ratios of leaf reflectances in narrow wavebands as indicators of plant stress," *Remote Sens.* **15**(3), 697–703 (1994).
73. J. P. Moore et al., "Adaptations of higher plant cell walls to water loss: drought vs desiccation," *Physiol. Plantarum* **134**(2), 237–245 (2008).
74. R. Jackson and C. Ezra, "Spectral response of cotton to suddenly induced water stress," *Int. J. Remote Sens.* **6**(1), 177–185 (1985).
75. W. B. Cohen, "Temporal versus spatial variation in leaf reflectance under changing water stress conditions," *Int. J. Remote Sens.* **12**(9), 1865–1876 (1991).
76. G. P. Badura et al., "A novel approach for deriving LAI of salt marsh vegetation using structure from motion and multiangular spectra," *IEEE J. Sel. Top. Appl. Earth Observ. Remote Sens.* **12**(2), 599–613 (2019).
77. M. Claverie et al., "Evaluation of medium spatial resolution BRDF-adjustment techniques using multi-angular SPOT4 (Take5) acquisitions," *Remote Sens.* **7**(9), 12057–12075 (2015).
78. N. Lu et al., "Estimation of nitrogen nutrition status in winter wheat from unmanned aerial vehicle based multi-angular multispectral imagery," *Front. Plant Sci.* **10**, 1601 (2019).
79. G. Bai et al., "NU-Spidercam: a large-scale, cable-driven, integrated sensing and robotic system for advanced phenotyping, remote sensing, and agronomic research," *Comput. Electron. Agric.* **160**, 71–81 (2019).
80. G. P. Asner and R. E. Martin, "Spectranomics: emerging science and conservation opportunities at the interface of biodiversity and remote sensing," *Glob. Ecol. Conserv.* **8**, 212–219 (2016).
81. J. Gamon et al., "Assessing vegetation function with imaging spectroscopy," *Surv. Geophys.* **40**, 489–513 (2019).
82. R.O. Chávez et al., "Modelling the spectral response of the desert tree Prosopis tamarugo to water stress," *Int. J. Appl. Earth Observ. Geoinf.* **21**, 53–65 (2013).
83. J. Hill, H. Buddenbaum, and P. A. Townsend, "Imaging spectroscopy of forest ecosystems: perspectives for the use of space-borne hyperspectral earth observation systems," *Surv. Geophys.* **40**(3), 553–588 (2019).
84. A. Comar et al., "ACT: a leaf BRDF model taking into account the Azimuthal anisotropy of monocotyledonous leaf surface," *Remote Sens. Environ.* **143**, 112–121 (2014).
85. X. Qian et al., "Exploring the potential of leaf reflectance spectra for retrieving the leaf maximum carboxylation rate," *Int. J. Remote Sens.* **40**(14), 5411–5428 (2019).

Biographies of the authors are not available.